Thin Solid Films 672 (2019) 26–32

Contents lists available at ScienceDirect

Thin Solid Films

journal homepage: www.elsevier.com/locate/tsf

An innovative approach for micro/nano structuring plasma polymer films

Damien Thiry[a,*], Nathan Vinx[a], Fancisco Javier Aparicio[b], David Moerman[c,d], Roberto Lazzaroni[c,d], Damien Cossement[d], Rony Snyders[a,d]

[a] Chimie des Interactions Plasma-Surface, CIRMAP, University of Mons, Place du Parc 20, B7000 Mons, Belgium
[b] Instituto de Ciencia de Materiales de Sevilla (CSIC-Universidad de Sevilla), Seville E-41092, Spain
[c] Laboratory for Chemistry of Novel Materials, CIRMAP, University of Mons, Place du Parc 20, B7000 Mons, Belgium
[d] Materia Nova Research Center, Parc Initialis, Avenue Nicolas Copernic 1, B-7000 Mons, Belgium

ARTICLE INFO

Keywords:
Plasma polymer
Nano-architecture
Bilayer
Substrate temperature

ABSTRACT

This work aims at presenting an innovative method for tailoring the morphology of functionalized plasma polymer films (PPF). The approach is based on the formation of a plasma polymer bilayer system in which the two layers differ by their chemical composition and cross-linking degree. As a case study, propanethiol-based plasma polymer films have been investigated. As revealed by a much higher S/C ratio than in the propanethiol precursor (i.e. 0.83 vs 0.33), it has been demonstrated that the bottom layer contains a large fraction of trapped sulfur-based molecules (e.g. H_2S). When further covered by a denser PPF formed at higher energetic conditions, a three-dimensional morphological reorganization takes place giving rise to the micro/nano structuration of the organic material. The shape, the dimensions as well as the density of the generated structures are found to depend on the thickness of both coatings involved in the bilayer structure, offering a great flexibility for surface engineering. Annealing experiments unambiguously confirm the major role played by the sulfur-based trapped molecules for inducing the reshaping process. The whole set of data clearly paves the way for the development of an innovative approach for finely tailoring the morphology of functionalized PPF at the micro/nano scale.

1. Introduction

Since 1980s, functionalized plasma polymer film (PPF) containing chemical groups such as $-NH_2$ [1,2], $-OH$ [3,4], $-COOH$ [5,6] and $-SH$ [7,8] have been given a considerable attention. Particularly, by taking benefit of the selective reactivity of the organic groups, such functional surface represents an adequate platform for specifically anchoring biomolecules (e.g. DNA, proteins) and cells [9–11], which is of prime importance for the fabrication of biosensors or in disease diagnosis [12,13].

Briefly, the plasma polymerization method is based on the activation of an organic precursor dosed into the plasma resulting from the formation of ions and neutral species (including radicals) and their subsequent condensation on exposed surfaces allowing for the growth of the solid film. The associated complex growth mechanism, which includes a multitude of gas phases and surface reactions pathways is responsible for the singular properties of PPF such as, for instance, the absence of repeating units in comparison with conventional polymers, their unique resistance to solvents and heat as well as their good adhesion properties on almost all kind of substrates [14–17].

It has been extensively reported for several functionalized PPF families (i.e. oxygen, nitrogen and sulfur-based ones) that, under certain experimental synthesis conditions, low molecular weight-oligomers and/or stable molecules, are embedded in the plasma polymer matrix [7,9,18–21]. The presence of these trapped species is responsible for prejudicial phenomena, especially in the context of biological applications requiring the immersion of the coatings in solution. For instance, the embedded molecules could be released in solution, initiating undesirable effects on the biological response of the material and thus jeopardizing the intended application [20,22,23]. Therefore, numerous efforts were made in the past to avoid the presence of trapped species in the material by using suitable experimental conditions. This work aims at showing that it is possible to take benefit from the presence of these unbound molecules for inducing a controlled structural reorganization of the material. The objective is to be able to modulate the micro/nano architecture of functionalized PPF, which is nowadays still highly challenging [24]. It is important to note that structuring at the micro/nano scale the architecture of functionalized organic-based thin films confers to the material unprecedented physico-chemical properties appealing for several technological applications including the modulation of the biological response of a material [25], the fabrication of super-hydrophobic coating [26] or highly sensitive biosensors [27], ….

* Corresponding author.
E-mail address: damien.thiry@umons.ac.be (D. Thiry).

https://doi.org/10.1016/j.tsf.2018.12.050
Received 29 August 2018; Received in revised form 31 December 2018; Accepted 31 December 2018
Available online 02 January 2019

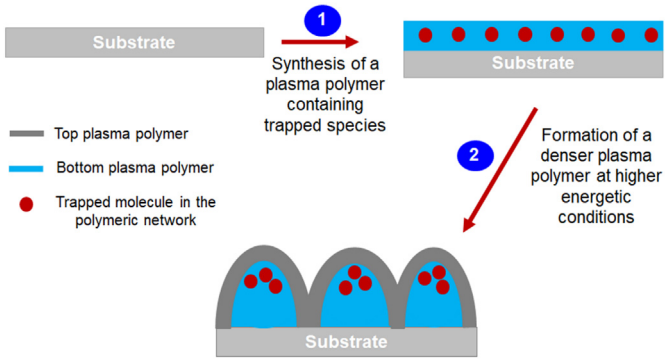

Scheme 1. Overall strategy developed in this work consisting, at first, in the synthesis of a PPF containing trapped molecules followed by the formation of a second denser PPF.

Most of the approaches reported in the literature for the deposition of structured plasma polymer surfaces are based on complex multistage processes involving rough and/or structured substrates templates fabricated by other techniques and/or post deposition processes [24,28]. Although the straightforward fabrication of structured fluorocarbon-based PPF has also been studied [26], for other precursors, the formation of morphological features has only been observed during the initial growth stages and thus limited to ultra-thin films [29].

In this context, a simple and direct method within the premises of a one-reactor approach for the deposition of nano/micro structured PPFs without the need of a patterned substrate is presented in this work. As it is schematically described in Scheme 1, this strategy is based on the deposition of a bilayer system constituted by two PPF differing by their chemical composition and cross-linking degree in order to control the morphology of functionalized PPF. To illustrate the simplicity of the proposed method in this work, the two depositions steps have been carried out in the same reactor by using the same organic precursor. The first step consisted in the synthesis of a propanethiol-based PPF containing a significant amount of trapped species. The choice of the propanethiol precursor was motivated by our previous works revealing that a large fraction of sulfur-based molecules (e.g. H_2S) can be embedded in the polymeric network under certain experimental conditions [7,18,19,30–32]. In the second step, a PPF acting as a barrier coating (and therefore synthesized in higher energetic conditions) has been deposited on the bottom layer. The idea behind this approach was to activate the outward diffusion of the trapped molecules for inducing the structural deformation of the material and giving rise to a nano/micro structured PPF. In order to evaluate the control that our strategy provides on the morphological characteristics of PPF, the influence of the thickness of both the bottom and the top layers has been investigated. Additionally, several fundamental aspects regarding the reshaping mechanism have also been addressed.

2. Experimental part

Propanethiol (Sigma Aldrich, 99% purity) has been plasma polymerized on 2 × 2 cm^2 Si wafers (110). Before their introduction into the chamber, the substrates have been washed in isopropanol.

The depositions have been carried out in a metallic vacuum chamber: 65 cm in length and 35 cm in diameter. The reactor has been pumped down by a combination of turbomolecular and primary pumps allowing to reach a residual pressure lower than 2×10^{-4} Pa. More details about the deposition chamber can be found elsewhere [18,32]. For all the PPF syntheses, the working pressure, controlled by a throttle valve connected to a capacitive gauge, has been fixed at 5.33 Pa. The plasma has been generated by using a one-turn inductive water-cooled copper coil (10 cm in diameter) located inside the chamber. The coil has been connected to an Advanced Energy RF (13.56 MHz) power supply via a matching network. The precursor flow rate has been fixed for all the experiments at 10 sccm. During the film depositions, the substrate was at the floating potential.

The deposition of plasma polymer bilayer has been made in the same reactor by switching two different plasma conditions without extinguishing the discharge. For the formation of the bottom PPF, the substrate temperature has been accurately regulated at 10 °C by combining a liquid nitrogen cooling system with an ohmic heating circuit. The power applied to the coil (P_{RF}) and the distance between the substrate and the plasma source have been fixed at 40 W and 10 cm, respectively. For the synthesis of the second PPF, P_{RF} has been increased to 100 W whereas the distance between the coil and the substrate was reduced to 2 cm. During that second step, the substrate temperature has been no longer controlled and has reached 30–35 °C at the end of the deposition. The influence of the thickness of the bottom PPF has been investigated from 58 nm to 350 nm (i.e. deposition time from 5 to 30 min) while the thickness of the top PPF in the range 53–320 nm (i.e. deposition time from 30 s to 2 min).

XPS (X-Ray Photoelectron Spectroscopy) measurements have been performed by using a PHI 5000 VersaProbe apparatus connected under vacuum to the deposition chamber. A monochromatized Al Kα line (1486.6 eV) has been used as the photon source. The atomic relative concentration of each element has been calculated from peaks areas taking into account the respective photoionization cross-sections, the electron inelastic mean free path, and the transmission function of the spectrometer.

Static time-of-flight secondary ion mass spectrometry (ToF-SIMS) measurements have been acquired using a ToF-SIMS IV instrument from IONTOF GmbH. A 10 keV Ar^+ ion beam has been used at a current of 0.75 pA rastered over a scan area of 300 × 300 μm^2 for 125 s. The spectra have been acquired in positive mode.

Cross-section scanning electron microscopy (SEM) imaging has been carried out on a FEG-SEM Hitachi SU8020 microscope operating at 3 kV. Prior to their analysis, the samples have been metallized by a 5 nm thick carbon-based coating and cleaved by using a diamond tip.

The AFM (Atomic Force Microscope) measurements have been carried out in controlled environment ($[O_2] < 5$ ppm and $[H_2O] < 1$ ppm), with a Bruker Multimode microscope equipped with a Nanoscope VIII controller. The microscope was operated in intermittent-contact mode, using commercially available silicon tips with a resonance frequency of about 300 kHz and a typical radius of curvature in the 5–10 nm range. The images are shown as recorded, except for a planefitting processing. The analysis of the AFM images has been performed by using “Nanoscope Analysis” software.

3. Results

Our research strategy has involved the formation of a bilayer system composed by two propanethiol plasma polymer films (Pr-PPF) synthesized in different experimental conditions. The choice of the experimental window for the synthesis of the bottom layer (i.e. substrate temperature fixed at 10 °C and P_{RF} = 40 W) has been made according to a previous work which has thoroughly investigated the influence of the thermal conditions of the substrate on the chemical composition as well as the cross-linking density of Pr-PPF [30]. It can be learned that cooling down the substrate favors the trapping of sulfur-based molecules (e.g. H_2S) within the PPF matrix. Following the formation of the bottom layer, a second Pr-PPF has been synthesized at higher energy input (i.e. from 40 to 100 W) while decreasing the distance between the substrate and the plasma source (i.e. from 10 to 2 cm). We are expecting that such a change in the conditions will activate the outward migration of the embedded molecules contained in the bottom layer; simultaneously, a denser upper PPF will form which is likely to lower the release of the diffusing species into the atmosphere.

Before examining the bilayer system in details, the chemical composition, the cross-linking degree and the morphology of both coatings

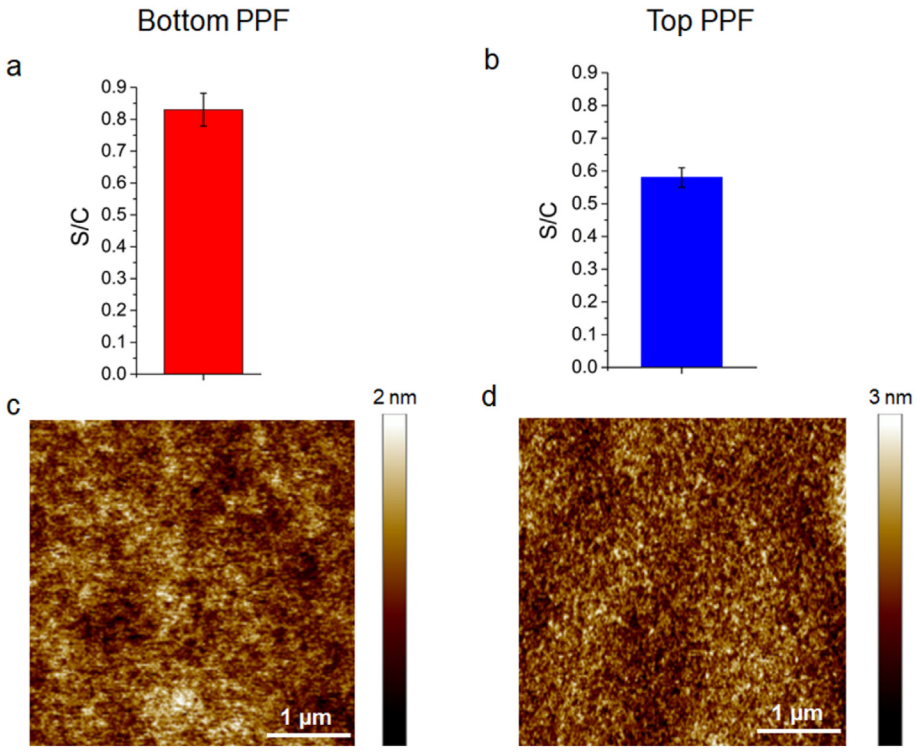

Fig. 1. S/C ratio measured by XPS for (a) the bottom and (b) the top PPF deposited as a single layer on silicon substrate and the corresponding 2D AFM images (c, d).

deposited as a single layer on silicon substrates have been investigated (Fig. 1). Regarding the chemical composition, the sulfur to carbon ratio (S/C) measured by XPS strongly differs depending on the synthesis conditions (Fig. 1a and b). For the low- energy-deposited PPF, the S/C ratio is much higher than in the propanethiol precursor (i.e. 0.83 vs 0.33). As previously reported, this behavior is attributed to the presence of unbound sulfur-based molecules (i.e. H_2S) in the polymer network [7,30–32]. On the other hand, the high- energy-deposited PPF shows a lower S/C ratio (i.e. 0.58), revealing that in this case the proportion of trapped species is significantly reduced. This trend can be explained by the lower production of H_2S species in the plasma, as reported by mass spectrometry measurements limiting therefore the trapping scenario [30].

To thoroughly characterize the physico-chemical properties of both PPF, ToF-SIMS experiments have been carried out. This technique has been proved to provide information about the cross-linking degree of the layers [33,34]. Fig. 2 represents the ToF-SIMS spectra recorded for the analysis of the two samples illustrating the high complexity of the data as testified by the numerous recorded peaks. Regarding the cross-linking degree, it has been reported that this parameter is inversely correlated to the total secondary ions intensity [33,34]. In our experimental window, a total secondary ion intensity of 38 965 ± 3446 (arbitrary unit) has been found for the low energy conditions in comparison to 22 344 ± 964 for the high-energy-deposited PPF. This unambiguously indicates an increase in the cross-linking density of the plasma polymer when shifting from the low to the high energy conditions as expected from the literature [1,35].

With regard to their morphology, both PPF are essentially smooth (average roughness of ~0.2 nm for both layers) as typically reported for PPF (Fig. 1c and d) [29,36].

When the two PPF are synthesized in the same conditions but are involved in a bilayer system, the resulting morphology strongly differs, as shown in Figs. 3 and 4: a micro/nano structuration is clearly identified revealing that a morphological reorganization occurs. The size, the shape as well as the density of the micro/nano objects are found to depend on the thickness of both coatings involved in the layered

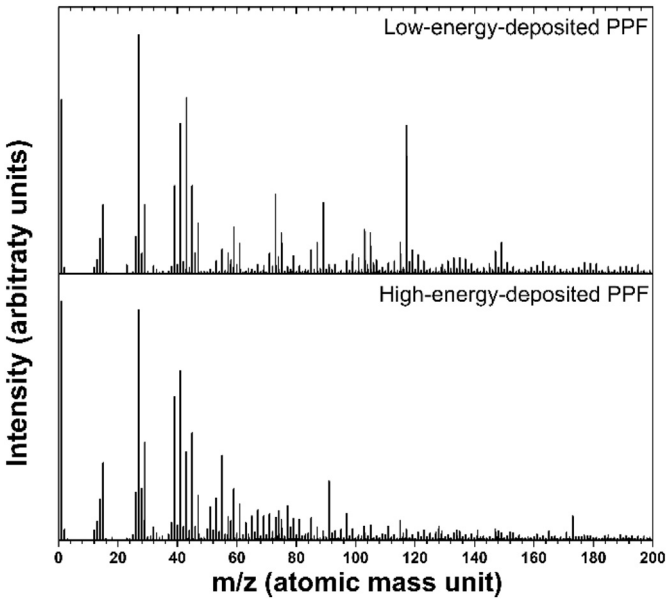

Fig. 2. Typical ToF-SIMS spectra of PPF synthesized for the low and high energetic conditions.

structure (Figs. 3 and 4).

In Fig. 3, it can be shown that for a given thickness of the top layer (i.e. t_t = 160 nm), the diameter (i.e. from ~200 ± 75 nm to 3100 ± 750 nm) as well as the height (i.e. from ~45 ± 20 nm to 800 ± 200 nm) of the structures exhibiting a dome-like shape increase with the thickness of the bottom PPF (t_b). Concomitantly, the density of the micro/nano objects is found to decrease when increasing t_b.

With regard to the influence of the thickness of the top layer (for t_b fixed at 350 nm), the shape of the micro/nano objects is found to evolve from a worm-like (with a length of ~2500 ± 1100 nm, a width of ~1100 ± 360 nm and a height of ~240 ± 70 nm) to a dome-like

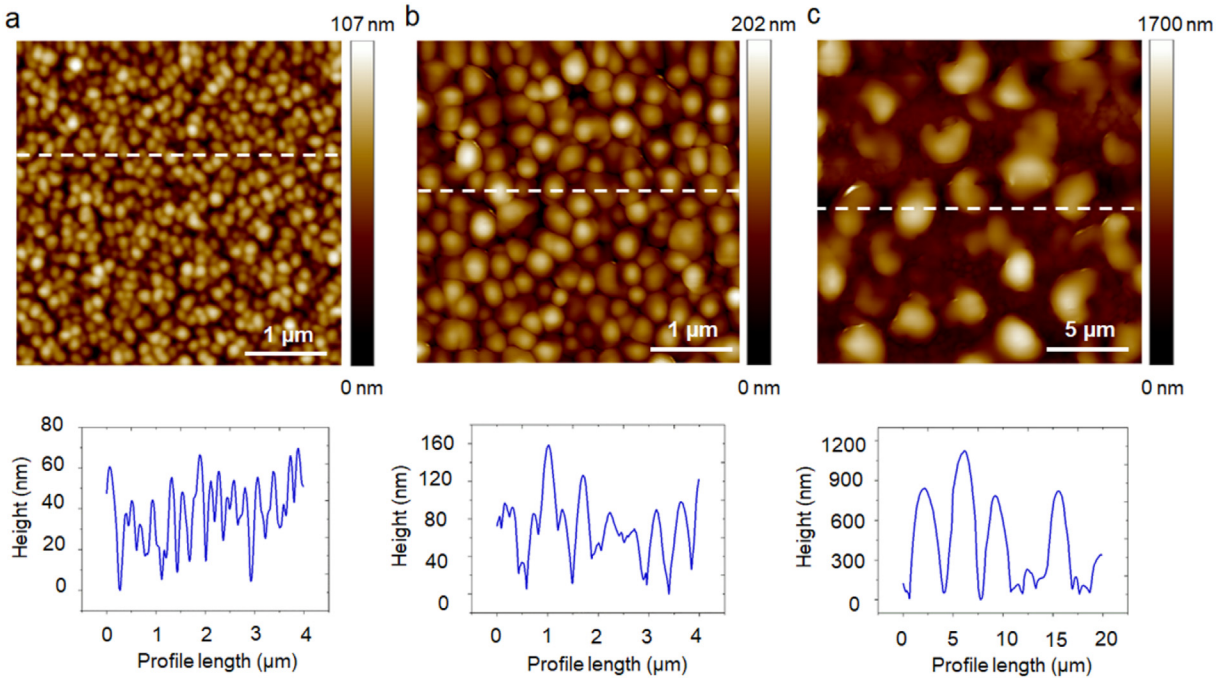

Fig. 3. 2D AFM and the corresponding line scans images of a bilayer Pr-PPF varying the thickness of the bottom layer: (a) 58 nm, (b) 175 nm and (c) 350 nm. The thickness of the top layer is fixed at 160 nm.

(with a diameter of ~3100 ± 750 nm and a height of ~800 ± 200 nm) and then to crescent–like structure (with a length of ~2500 ± 1100 nm, a width of ~2000 ± 900 nm and a height of ~1450 ± 300 nm) when increasing t_t from 53 to 320 nm (Fig. 4). Also, in this case, the density of the particles decreases when increasing the thickness.

In order to evaluate if the deformation of the bottom layer takes place over the whole thickness, cross-section SEM imaging has been carried out (Fig. 5). It can be shown that the nano/micro objects stand on a flat PPF presenting a thickness of about 200 nm.

At this stage, a major advantage of our methodology can be pointed out. Thanks to our strategy, nano/micro functionalized PPF can be obtained with a large control over the dimension of the structures (i.e. from the nano to the micrometer scale) by simply adjusting the thickness of both thin films involved in the bilayer system. Based on our experimental observations and considering the growth of PPF at a molecular level, a scenario can be tentatively proposed, as schematically shown in Fig. 6. First of all, as previously mentioned, a large density of unbound stable molecules (e.g. H_2S) is trapped in the bottom layer. At the initial stage of the growth of the second PPF, a higher level

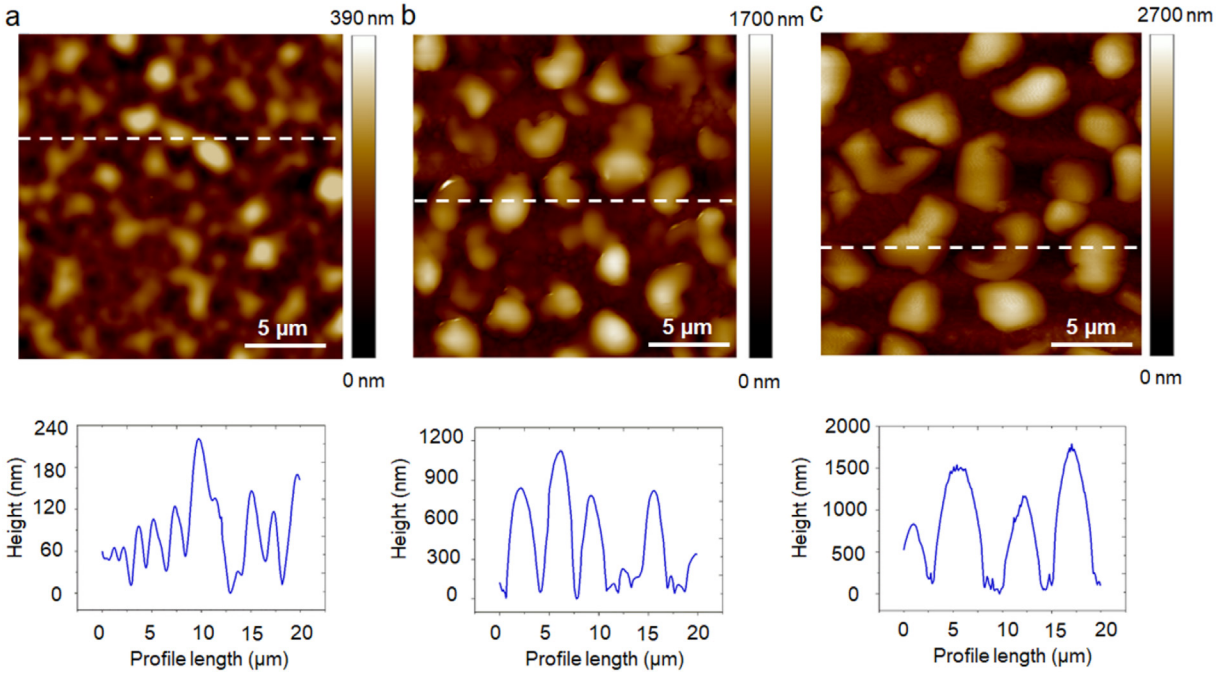

Fig. 4. 2D AFM and the corresponding line scans images of a bilayer Pr-PPF varying the thickness of the top layer: (a) 53 nm, (b) 160 nm and (c) 320 nm. The thickness of the bottom layer is fixed at 350 nm.

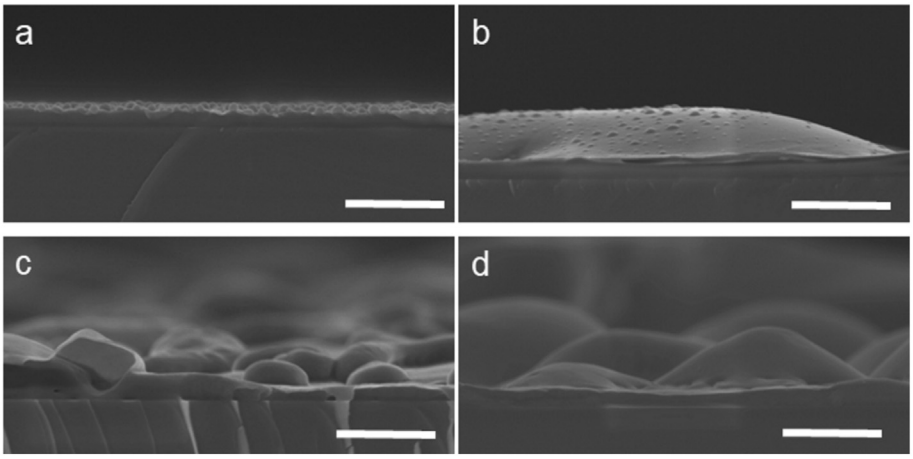

Fig. 5. Cross-section SEM images of a bilayer Pr-PPF varying the thickness of the bottom layer (thickness of the top layer fixed at 160 nm): (a) 58 nm (b) 350 nm. Cross-section SEM images of a bilayer Pr-PPF varying the thickness of the top layer (thickness of the bottom layer fixed at 350 nm): (c) 53 nm (d) 320 nm. Scale bar: 1 μm.

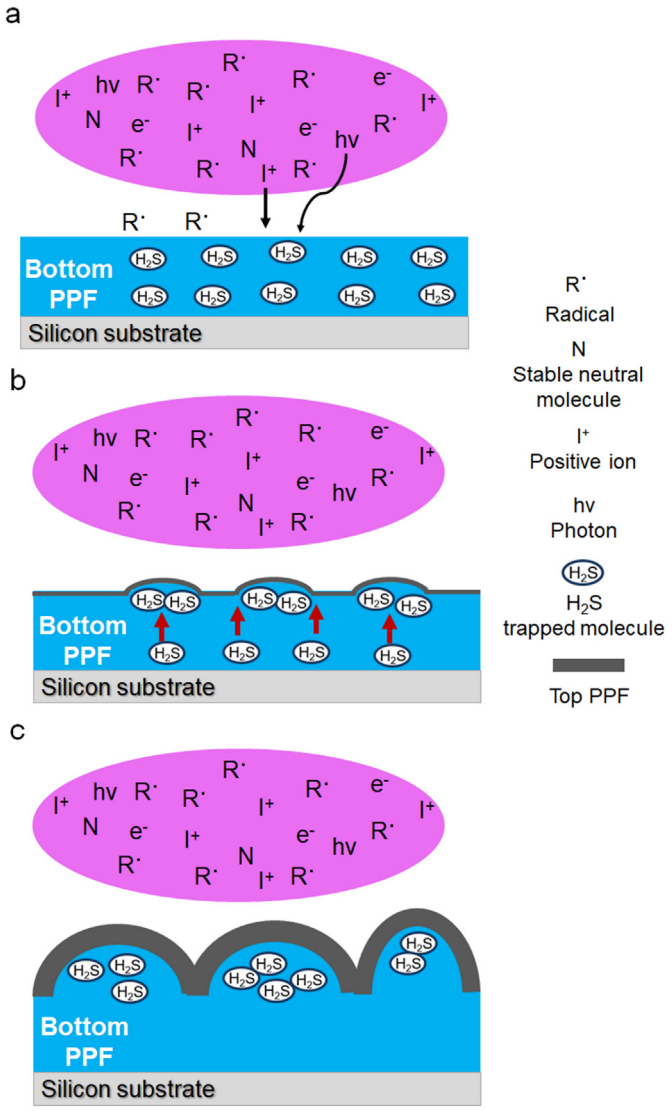

Fig. 6. Scenario explaining the reorganization of the bilayered PPF. See the text for more details.

of energy is transferred to the already deposited bottom layer through several surface processes including ion impact, photon irradiation and exothermic radicals chemisorption reaction (Fig. 6a) [37]. Indeed, it has been reported that the increase in the energy dissipated in the discharge and the reduced distance between the plasma source and the substrate results in an increase in the ion flux and photon irradiation toward the growing film [31,38,39]. On the other hand, the contribution of exothermic surface reactions is directly related to the kinetic of deposition [31,37]. In our experimental window, the deposition rate when switching from the low to higher energetic conditions has significantly increased from ~15 nm/min to ~320 nm/min. Therefore, for a given period of time, a higher number of exothermic condensation reactions occur, contributing to increase the energy flux toward the interface.

This energy load to the bottom PPF is likely to induce an increase in the surface temperature thereby activating the outward diffusion of the trapped H_2S species present in the bottom layer. Meanwhile, the second PPF is growing as a function of time. As this second PPF presents a more cross-linked polymer network, this material could therefore act as a barrier coating lowering the outward migration of the embedded molecules. The concomitant outward diffusion of molecules and the formation of the denser upper PPF could result in the observed three-dimensional expansion of the material (Fig. 6b). Furthermore, according to the Laplace law, the formation of a curved surface significantly increases the internal pressure providing additional driving force for inducing the deformation of the polymeric material [40]. At the final stage, an organic-based micro/nano structured material constituted by a deformed PPF containing embedded species covered by a second PPF is formed (Fig. 6c). From this mechanism, the influence of the thickness of the bottom coating as observed experimentally can be understood as follows: increasing the thickness results in an increase in the absolute amount of the trapped species giving rise to a more pronounced tridimensional deformation of the material. Consequently, the objects become larger in size while their density decreases. Because of the top PPF covers the plasma polymer particles, its thickness also directly affects the height as well as the lateral dimension of the nano/micro objects.

In order to validate the proposed structuration mechanism, two extra experiments have been carried out. The first one has consisted in annealing the bottom layer during 1 h in air at 200 °C before the deposition of the denser PPF. As shown in Fig. 7, the formation of micro/nano organized PPF hasn't occurred in that case. Interestingly, a drastic decrease in the S/C ratio has been observed after annealing likely due to the outward diffusion of the sulfur-based embedded species into the atmosphere.

A similar thermal treatment has also been applied to a bilayered structured PPF. As shown in Fig. 8 a and b, a dramatic decrease in the height of the particles (i.e. by ~90%) has occurred whereas their diameter remained almost unchanged. This behavior can be explained by the activated migration in the atmosphere of the embedded species, as confirmed by the large decrease in the S/C ratio after annealing (Fig. 8c).

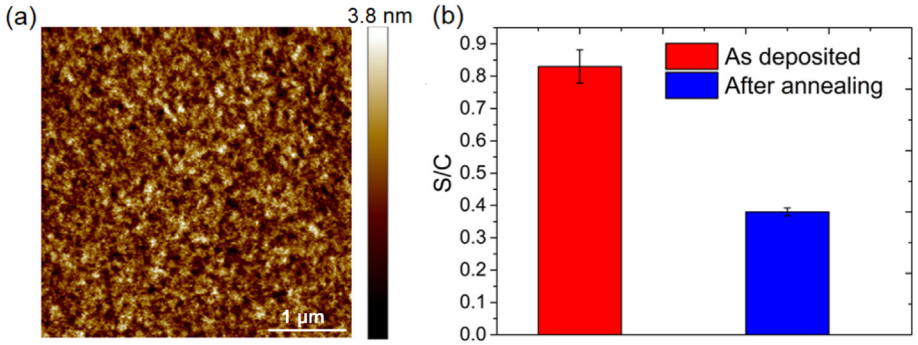

Fig. 7. (a) 2D AFM image of a bilayer Pr-PPF formed by a bottom coating (350 nm) previously annealed at 200 °C during 1 h prior the deposition of a top layer of 320 nm. (b) Evolution of the S/C ratio measured by XPS for the bottom Pr-PPF synthesized before and after annealing in air during 1 h at 200 °C.

The overall set of data regarding the influence of the annealing procedure therefore unambiguously confirms the key role of the embedded species in the bottom layer for activating the reshaping process.

4. Conclusion

In this work, an innovative strategy aiming at controlling the micro/nano architecture of sulfur-based plasma polymer films has been established. Our approach has consisted in the synthesis of a deformable plasma polymer containing a large proportion of trapped species which, when further covered by an additional denser plasma polymer, has undergone a morphological reorganization. The fundamental reshaping mechanism, as confirmed by several complementary experimental results, involves the activation of the outward diffusion of the trapped molecules during the growth of the top plasma polymer formed at higher energy and acting as a barrier layer.

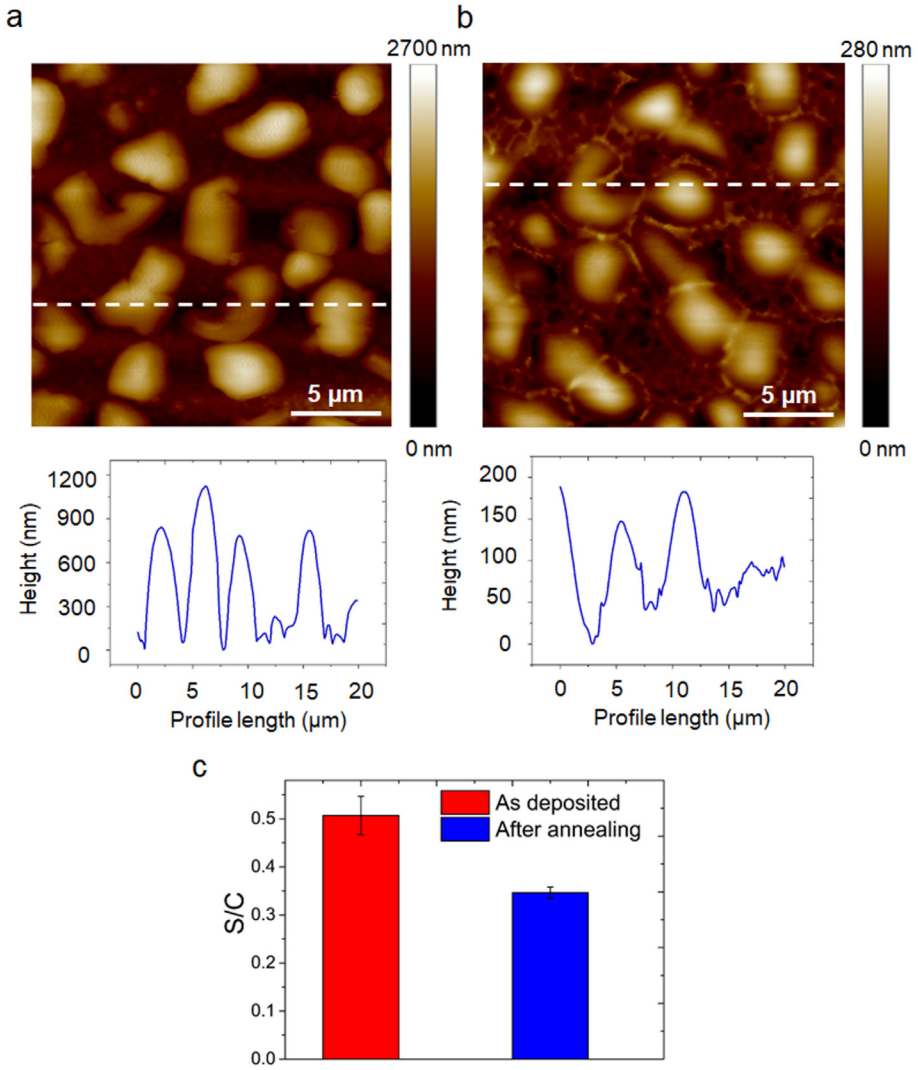

Fig. 8. 2D AFM and the corresponding line scans images of a bilayer Pr-PPF formed by a bottom (350 nm) and top (320 nm) coatings (a) before and (b) after annealing in the air at 200 °C during 1 h. (c) Evolution of the corresponding S/C ratio measured by XPS before and after annealing.

The attractiveness of our method lies in the easiness to tailor the shape (e.g. dome-like, worm-like, …) and the dimensions (i.e. from ~50 nm to ~3500 nm) of the plasma polymer pattern by modulating the thickness of the coatings involved in the bilayer system. This high flexibility paves the way for the fabrication of tailor-made organic-based coatings with a tunable morphology appealing for numerous applications, especially in the biotechnology field (e.g. for driving the response of the material toward cells interaction). Furthermore, owing to the good adhesion properties of plasma polymers, this strategy can in principle be applied to almost all kind of substrates.

Finally, it has to be mentioned that the presence of embedded stable molecules in plasma polymeric network has until now always been considered as a serious problem. This work shows how to benefit of this feature to control the morphology of plasma polymer films opening the door to further developments in the field.

Acknowledgements

The authors are grateful to Prof. P. Damman (University of Mons, Belgium) for the fruitful discussions about the reshaping mechanism. D. Thiry would like to thank the “Région Wallone” through the CLEANAIR project for its financial support. D. Moerman is grateful to FNRS for a postdoctoral fellowship and for its support through the ECOSTOFLEX project.

References

[1] L. Denis, D. Thiry, D. Cossement, P. Gerbaux, F. Brusciotti, I. Van De Keere, V. Goossens, H. Terryn, M. Hecq, R. Snyders, Towards the understanding of plasma polymer film behaviour in ethanol: a multi-technique investigation, Prog. Org. Coat. 70 (2011) 134–141, https://doi.org/10.1016/j.porgcoat.2010.11.006.
[2] A. Choukourov, H. Biederman, D. Slavinska, L. Hanley, A. Grinevich, H. Boldyryeva, A. Mackova, Mechanistic studies of plasma polymerization of allylamine, J. Phys. Chem. B 109 (2005) 23086–23095, https://doi.org/10.1021/jp0535691.
[3] C.L. Rinsch, X. Chen, V. Panchalingam, R.C. Eberhart, J.-H. Wang, R.B. Timmons, Pulsed radio frequency plasma polymerization of allyl alcohol: controlled deposition of surface hydroxyl groups, Langmuir 12 (1996) 2995–3002, https://doi.org/10.1021/la950685u.
[4] L. Watkins, A. Bismarck, A.F. Lee, D. Wilson, K. Wilson, An XPS study of pulsed plasma polymerised allyl alcohol film growth on polyurethane, Appl. Surf. Sci. 252 (2006) 8203–8211, https://doi.org/10.1016/j.apsusc.2005.10.045.
[5] S.A. Voronin, M. Zelzer, C. Fotea, M.R. Alexander, J.W. Bradley, Pulsed and continuous wave acrylic acid radio frequency plasma deposits: plasma and surface chemistry, J. Phys. Chem. B 111 (2007) 3419–3429, https://doi.org/10.1021/jp068488z.
[6] R. Jafari, M. Tatoulian, W. Morscheidt, F. Arefi-Khonsari, Stable plasma polymerized acrylic acid coating deposited on polyethylene (PE) films in a low frequency discharge (70kHz), React. Funct. Polym. 66 (2006) 1757–1765, https://doi.org/10.1016/j.reactfunctpolym.2006.08.006.
[7] D. Thiry, R. Francq, D. Cossement, M. Guillaume, J. Cornil, R. Snyders, A detailed description of the chemistry of thiol supporting plasma polymer films, Plasma Process. Polym. 11 (2014) 606–615, https://doi.org/10.1002/ppap.201400015.
[8] E. Kasparek, D. Thiry, J.R. Tavares, M.R. Wertheimer, R. Snyders, P.-L. Girard-Lauriault, Growth mechanisms of sulfur-rich plasma polymers: binary gas mixtures versus single precursor, Plasma Process. Polym. (2018), https://doi.org/10.1002/ppap.201800036.
[9] R. Förch, Z. Zhang, W. Knoll, Soft plasma treated surfaces: tailoring of structure and properties for biomaterial applications, Plasma Process. Polym. 2 (2005) 351–372, https://doi.org/10.1002/ppap.200400083.
[10] S. Liu, M.M.L.M. Vareiro, S. Fraser, A.T.A. Jenkins, Control of attachment of bovine serum albumin to pulse plasma-polymerized maleic anhydride by variation of pulse conditions, Langmuir 21 (2005) 8572–8575, https://doi.org/10.1021/la051449e.
[11] K.S. Siow, L. Britcher, S. Kumar, H.J. Griesser, Plasma methods for the generation of chemically reactive surfaces for biomolecule immobilization and cell colonization – a review, Plasma Process. Polym. 3 (2006) 392–418, https://doi.org/10.1002/ppap.200600021.
[12] L. Jin, A. Horgan, R. Levicky, Preparation of end-tethered DNA monolayers on siliceous surfaces using heterobifunctional cross-linkers, Langmuir 19 (2003) 6968–6975, https://doi.org/10.1021/la034461k.
[13] A. Misra, P. Dwivedi, Immobilization of oligonucleotides on glass surface using an efficient heterobifunctional reagent through maleimide–thiol combination chemistry, Anal. Biochem. 369 (2007) 248–255, https://doi.org/10.1016/j.ab.2007.05.027.
[14] D. Thiry, S. Konstantinidis, J. Cornil, R. Snyders, Plasma diagnostics for the low-pressure plasma polymerization process: a critical review, Thin Solid Films 606 (2016) 19–44, https://doi.org/10.1016/j.tsf.2016.02.058.
[15] J. Friedrich, Mechanisms of plasma polymerization – reviewed from a chemical point of view, Plasma Process. Polym. 8 (2011) 783–802, https://doi.org/10.1002/ppap.201100038.
[16] A. Choukourov, P. Pleskunov, D. Nikitin, V. Titov, A. Shelemin, M. Vaidulych, A. Kuzminova, P. Solař, J. Hanuš, J. Kousal, Advances and challenges in the field of plasma polymer nanoparticles, Beilstein J. Nanotechnol. 8 (2017) 2002, https://doi.org/10.3762/bjnano.8.200.
[17] M. Vandenbossche, D. Hegemann, Recent approaches to reduce aging phenomena in oxygen-and nitrogen-containing plasma polymer films: an overview, Curr. Opin. Solid State Mater. Sci. 22 (2018) 26–38, https://doi.org/10.1016/j.cossms.2018.01.001.
[18] D. Thiry, N. Britun, S. Konstantinidis, J.-P. Dauchot, M. Guillaume, J. Cornil, R. Snyders, Experimental and theoretical study of the effect of the inductive-to-capacitive transition in propanethiol plasma polymer chemistry, J. Phys. Chem. C 117 (2013) 9843–9851, https://doi.org/10.1021/jp400829z.
[19] D. Thiry, N. Britun, S. Konstantinidis, J.-P. Dauchot, L. Denis, R. Snyders, Altering the sulfur content in the propanethiol plasma polymers using the capacitive-to-inductive mode transition in inductively coupled plasma discharge, Appl. Phys. Lett. 100 (2012) 071604, , https://doi.org/10.1063/1.3686902.
[20] K. Vasilev, L. Britcher, A. Casanal, H.J. Griesser, Solvent-induced porosity in ultrathin amine plasma polymer coatings, J. Phys. Chem. B 112 (2008) 10915–10921, https://doi.org/10.1021/jp803678w.
[21] M. Alexander, T. Duc, The chemistry of deposits formed from acrylic acid plasmas, J. Mater. Chem. 8 (1998) 937–943, https://doi.org/10.1039/A708064F.
[22] L.-Q. Chu, W. Knoll, R. Förch, Stabilization of plasma-polymerized allylamine films by ethanol extraction, Langmuir 22 (2006) 5548–5551, https://doi.org/10.1021/la0606392.
[23] Z. Zhang, B. Menges, R. Timmons, W. Knoll, R. Förch, Surface plasmon resonance studies of protein binding on plasma polymerized di (ethylene glycol) monovinyl ether films, Langmuir 19 (2003) 4765–4770, https://doi.org/10.1021/la026980d.
[24] D. Thiry, A. Chauvin, A.-A. El Mel, C. Cardinaud, J. Hamon, E. Gautron, N. Stephant, A. Granier, P.-Y. Tessier, Tailoring the chemistry and the nano-architecture of organic thin films using cold plasma processes, Plasma Process. Polym. 14 (2017) 1700042, , https://doi.org/10.1002/ppap.201700042.
[25] Z. Chen, A. Bachhuka, S. Han, F. Wei, S. Lu, R.M. Visalakshan, K. Vasilev, Y. Xiao, Tuning chemistry and topography of nanoengineered surfaces to manipulate immune response for bone regeneration applications, ACS Nano 11 (2017) 4494–4506, https://doi.org/10.1021/acsnano.6b07808.
[26] R. Di Mundo, R. Gristina, E. Sardella, F. Intranuovo, M. Nardulli, A. Milella, F. Palumbo, R. d'Agostino, P. Favia, Micro-/nanoscale structuring of cell-culture substrates with fluorocarbon plasmas, Plasma Process. Polym. 7 (2010) 212–223, https://doi.org/10.1002/ppap.200900112.
[27] A. Artemenko, H. Kozak, H. Biederman, A. Choukourov, A. Kromka, Amination of NCD films for possible application in biosensing, Plasma Process. Polym. 12 (2015) 336–346, https://doi.org/10.1002/ppap.201400151.
[28] O. Kylián, A. Choukourov, H. Biederman, Nanostructured plasma polymers, Thin Solid Films 548 (2013) 1–17, https://doi.org/10.1016/j.tsf.2013.09.003.
[29] A. Michelmore, P. Martinek, V. Sah, R.D. Short, K. Vasilev, Surface morphology in the early stages of plasma polymer film growth from amine-containing monomers, Plasma Process. Polym. 8 (2011) 367–372, https://doi.org/10.1002/ppap.201000140.
[30] F.J. Aparicio, D. Thiry, P. Laha, R. Snyders, Wide range control of the chemical composition and optical properties of propanethiol plasma polymer films by regulating the deposition temperature, Plasma Process. Polym. 13 (2016) 814–822, https://doi.org/10.1002/ppap.201500212.
[31] D. Thiry, F.J. Aparicio, P. Laha, H. Terryn, R. Snyders, Surface temperature: a key parameter to control the propanethiol plasma polymer chemistry, J. Vac. Sci. Technol. A 32 (2014) 050602, , https://doi.org/10.1116/1.4890672.
[32] D. Thiry, F.J. Aparicio, N. Britun, R. Snyders, Concomitant effects of the substrate temperature and the plasma chemistry on the chemical properties of propanethiol plasma polymer prepared by ICP discharges, Surf. Coat. Technol. 241 (2014) 2–7, https://doi.org/10.1016/j.surfcoat.2013.10.063.
[33] D. Thiry, M. Pouyanne, D. Cossement, A. Hemberg, R. Snyders, Surface engineering of bromine-based plasma polymer films: a step toward high thiol density-containing organic coatings, Langmuir 34 (2018) 7655–7662, https://doi.org/10.1021/acs.langmuir.8b01045.
[34] U. Oran, S. Swaraj, J.F. Friedrich, W.E. Unger, Surface analysis of plasma-deposited polymer films, 3, Plasma Process. Polym. 1 (2004) 141–152.
[35] D. Cossement, F. Renaux, D. Thiry, S. Ligot, R. Francq, R. Snyders, Chemical and microstructural characterizations of plasma polymer films by time-of-flight secondary ion mass spectrometry and principal component analysis, Appl. Surf. Sci. 355 (2015) 842–848, https://doi.org/10.1016/j.apsusc.2015.07.066.
[36] M. Vandenbossche, L. Petit, J. Mathon-Lagresle, F. Spano, P. Rupper, L. Bernard, D. Hegemann, Formation of lateral chemical gradients in plasma polymer films shielded by an inclined mask, Plasma Process. Polym. 15 (2018) 1700185, , https://doi.org/10.1002/ppap.201700185.
[37] H. Kersten, H. Deutsch, H. Steffen, G.M.W. Kroesen, R. Hippler, The energy balance at substrate surfaces during plasma processing, Vacuum 63 (2001) 385–431, https://doi.org/10.1016/s0042-207x(01)00350-5.
[38] A. Michelmore, C. Charles, R.W. Boswell, R.D. Short, J.D. Whittle, Defining plasma polymerization: new insight into what we should be measuring, ACS Appl. Mater. Interfaces 5 (2013) 5387–5391, https://doi.org/10.1021/am401484b.
[39] S. Saboohi, S.A. Al-Bataineh, H. Safizadeh Shirazi, A. Michelmore, J.D. Whittle, Continuous-wave RF plasma polymerization of furfuryl methacrylate: correlation between plasma and surface chemistry, Plasma Process. Polym. 14 (2017) 1600054, , https://doi.org/10.1002/ppap.201600054.
[40] G.A. Somorjai, Y. Li, Introduction to Surface Chemistry and Catalysis, John Wiley & Sons, New Jersey, 2010.